Superconducting micronets: The Wheatstone bridge

Christine Ammann and Paul Erdös
Institute of Theoretical Physics, University of Lausanne, CH-1015 Lausanne, Switzerland

Stephen B. Haley
Department of Electrical and Computer Engineering, University of California, Davis, California 95616
(Received 29 November 1994)

Using the Ginzburg-Landau theory, a particular superconducting (sc) micronet, called the Wheatstone bridge, is studied. This planar micronet is made of two nodes connected by three thin sc wires. A magnetic field is applied perpendicularly to its plane. The sc-normal second-order phase transition is characterized by only two configurations of the order parameter: $\varphi_A = \varphi_B$ and $\varphi_A = -\varphi_B$, where φ_A and φ_B are the order parameters at the nodes. For temperatures near T_c, we show that only the $\varphi_A = \varphi_B$ configuration is admissible for fluxes near $\Phi = n\Phi_0$, where n is an integer and Φ_0 is the flux quantum. Finally, the exact solution of the nonlinear Ginzburg-Landau equations for one-dimensional systems is numerically fitted to the boundary conditions of the Wheatstone bridge for the two configurations $\varphi_A = \varphi_B$ and $\varphi_A = -\varphi_B$. Graphs of the Gibbs energy and of the spontaneous supercurrent, which for these two configurations is always a screening supercurrent, are given as functions of the total flux. A discontinuous transition between configurations occurs as a function of the flux.

I. INTRODUCTION

A superconducting (sc) micronet is a two-dimensional mesoscopic layout of multiply connected sc wires. For the uniform case, the wires are all identical and made of the same material. The radius of the wires is considered negligible with respect to the lengths of the branches. A node is a point where at least three wires join together and a branch is a segment of nodeless wire between two nodes. There is no discontinuity of the material at the nodes. A uniform magnetic field is applied perpendicularly to the plane of the micronet.

The study of this type of system was initiated in 1981 by de Gennes[1] who calculated the properties of the sc-normal second-order phase transition for the lasso (a ring with a dangling side branch) using the linearized mean-field Ginzburg-Landau formalism. Alexander,[2] Simonin *et al.*,[3] and Fink *et al.*[4] further developed this approach for different geometries (Sierpinski gasket, infinite microladder, etc.). Fink and Grünfeld[5] studied a wire with dangling side branches and examined[6,7] a new type of sc quantum interference device (SQUID) which functions without Josephson junctions. This device consists of a ring to which two diametrally opposite branches are connected, into which a transport current is injected.

In this paper, the Wheatstone bridge geometry is considered (see Fig. 1) using the nonlinear Ginzburg-Landau formalism. This micronet consists of three branches joining two nodes and may be considered as a first step in complexity after the ring and the lasso. It offers the possibility of exact numerical computation with a nontrivial behavior in the sc phase. Some results have been obtained by Fink[8] for a particular form of the Wheatstone bridge, called the yin-yang, where all three branches have the same length. In this paper, the spontaneous currents and the Gibbs energy are computed as functions of the temperature T and of the total magnetic flux Φ through one of the loops of the network. The phase diagram $\{T, \Phi\}$ is established. It will be seen that a first-order transition appears in the sc domain characterized by a sudden inversion of the direction of the currents.

II. GINZBURG-LANDAU THEORY

As we study the macroscopic properties of a system which is, by its nature, inhomogeneous (wires alternate with insulators), the phenomenological Ginzburg-Landau (GL) theory is the most appropriate tool to use. This theory attributes a change of Gibbs energy to the sc state with respect to the normal state of the form

$$G_s(A) - G_n(A) \equiv \Delta G(\varphi, A) = \xi^3 \int d^3x \left\{ \frac{|\alpha|^2}{\beta} \left(|\hat{p}\varphi|^2 - |\varphi|^2 + \frac{1}{2}|\varphi|^4 \right) + \frac{\mu_0}{2} H_{\text{ind}}^2 \right\}. \quad (1)$$

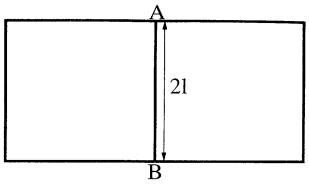

FIG. 1. Special geometry of the Wheatstone bridge where the ratio of the lengths of the lateral branches to that of the central branch is $\delta = 3$.

Here $\xi = \xi(T)$ is the coherence length of the material at temperature T; $x = \tilde{x}/\xi(T)$ is the normalized position vector, with $\tilde{x}$ the effective position vector; $\alpha \propto (T - T_c)$ and β are the two usual parameters of the GL theory (see Ref. 9); the normalized GL order parameter φ is defined by $\varphi(x) = \tilde{\varphi}(x)/\varphi_\infty$, with $\tilde{\varphi}$ the GL order parameter and $\varphi_\infty^2 = |\alpha|/\beta$; $H_{\rm ind}(x)$ is the magnetic field induced by the supercurrents in the micronet; m is the mass of a single electron; and $\hat{p}$ is a gauge-invariant momentum operator defined by

$$\hat{p} = -i\nabla - A, \tag{2}$$

where ∇ is the gradient operator for x and $A = (2\pi/\Phi_0)\tilde{A}$, with Φ_0 the unit flux quantum and $\tilde{A}$ a vector potential. The integration is carried out over the whole space. The first term in the parentheses of Eq. (1) is called the kinetic energy; the sum of the second and third terms is called the condensation energy.

Using a variational method for the variables φ and A, two equations, the Ginzburg-Landau equations, are derived from ΔG. The first of these,

$$\hat{p}^2\varphi - \varphi + |\varphi|^2\varphi = 0, \tag{3}$$

gives the value of φ, while the second one, not given here, combined with the Maxwell equation $\mathrm{curl}\, H = J^p$, ensures that if the supercurrent density is

$$J^p = -\frac{m\xi}{e|\varphi_\infty|^2\hbar}J, \tag{4}$$

with the normalized supercurrent density

$$J = \mathrm{Re}(\varphi^*\hat{p}\varphi), \tag{5}$$

then the total Gibbs energy is minimal with respect to variations in A. (Re means the real part of a complex expression.)

III. GENERAL SOLUTION OF THE GINZBURG-LANDAU EQUATION FOR ONE-DIMENSIONAL SYSTEMS

In micronets made of one-dimensional conductors such as wires, both φ and A become functions of the normalized curvilinear abscissa s. Then Eq. (3) must be solved with ∇ in $\hat{p}$ replaced by $\partial/\partial s$. We set

$$\varphi(s) = \sqrt{N(s)}e^{i[\theta(s)+\int A\cdot ds]}, \tag{6}$$

with N and θ real functions of s and $N \geq 0$. With this choice, the vector potential no longer appears explicitly in the equations for N and θ, and θ is gauge invariant. N is the squared modulus of the order parameter. We get, as a first result, that

$$J = N\theta', \tag{7}$$

where the prime denotes differentiation with respect to s. We choose to express $N(s)$ as

$$R(s) = N(s) - N_0, \tag{8}$$

where $N_0 = N(s_0)$, s_0 being a given abscissa. These definitions [Eqs. (6) and (8)], inserted in the Ginzburg-Landau equation (3), yield[10]

$$R'^2 = 2R(R^2 + 2a_0^2R + N_0'') + (N_0')^2 \tag{9}$$

and

$$J^2 = J_0^2 + \frac{N_0}{2}\left(N_0'' - \frac{(N_0')^2}{2N_0}\right), \tag{10}$$

with $N_0' = N'(s_0)$ and $N_0'' = N''(s_0)$,

$$a_0^2 = 3N_0/2 - 1 \tag{11}$$

and

$$J_0 = N_0\sqrt{1 - N_0}. \tag{12}$$

With the assumption that s_0 is so chosen that N_0 is an extremum of $N(s)$ (i.e. $N_0' = 0$), the solution of the general one-dimensional equation (9) is typically composed of Jacobian elliptic functions and its precise form depends on the values of the parameters N_0 and J as shown in Table I (Ref. 11) and Fig. 2. (The boundary conditions are not yet taken into account.) We use the definitions in Ref. 13 for the Jacobian elliptic functions and introduce

$$J_1 = \left(1 - \frac{N_0}{2}\right)\sqrt{\frac{N_0}{2}}. \tag{13}$$

Besides J_0 and J_1, the solutions depend on the two parameters

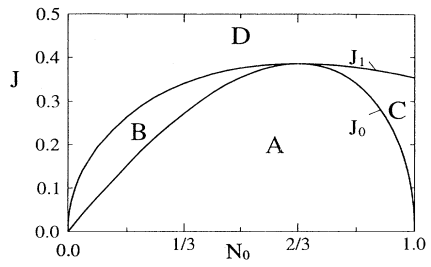

FIG. 2. Regions of validity of the different solutions of the GL equation for a one-dimensional superconductor. N_0 is the extremum of the normalized squared modulus of the sc order parameter. J is the normalized supercurrent. J_0 and J_1 are defined in Eqs. (12) and (13), respectively. The zones A, B, C, and D refer to Table I.

TABLE I. The different types of solutions of the normalized one-dimensional Ginzburg-Landau equation [Eq. (3)] for $R(s)$ defined by $N(s) = |\varphi|^2(s) = N_0 - R(s)$. The zones refer to the parameter space $\{N_0, J\}$ (see Fig. 2). $N_0 = N(s_0)$ is an extremum of $N(s)$, $N_0'' = N''(s_0)$ and $\varphi(s)$ is the normalized order parameter. The constants a_0, J_0, and J_1 and the parameters Δ^2 and $2\gamma^2$ are defined in the text [Eqs. (11)–(15)]. The Jacobian elliptic functions sd, sn, sc, and dn are defined in Ref. 13.

Zone	$\lvert J\rvert$	N_0	$R(s) = N(s) - N_0$	u	m
A	$\lvert J\rvert \le J_0$	arbitrary	$(2\gamma^4/\Delta^2)\mathrm{sd}^2(u\lvert m)$		
B	$J_0 \le \lvert J\rvert \le J_1$	$N_0 \le 2/3$	$2\gamma^4/[\Delta^2(1-m)]\mathrm{sn}^2[\sqrt{1-m}\,u\lvert m/(m-1)]$	Δs	$1/2(1+a_0^2/\Delta^2)$
C		$N_0 \le 2/3$	$2\gamma^4/(\Delta^2 m)\mathrm{sc}^2(\sqrt{m}\,u\lvert m^{-1})$		
D	$\lvert J\rvert > J_1$	arbitrary	$2\gamma^2\mathrm{sc}^2(u\lvert m)\mathrm{dn}^2(u\lvert m)$	γs	$1/2(1-a_0^2/2\gamma^2)$

$$\Delta^2 = \sqrt{2(J_1^2 - J^2)/N_0} \tag{14}$$

and

$$2\gamma^2 = \sqrt{N_0''} = \sqrt{\frac{2}{N_0}(J^2 - J_0^2) + \frac{(N_0')^2}{2N_0}}. \tag{15}$$

The last equality follows from Eq. (10).

Two cases have to be distinguished: (i) $N_0 \neq 0$ and (ii) $N_0 = 0$.

(i) If $N_0 \neq 0$, for any given values of N_0 and J, Eqs. (11)–(15) uniquely determine the two parameters Δ^2 and $2\gamma^2$ and, as $J_0 \le J_1$, a solution R is well defined. On the curve $J(N_0) = J_0$, R vanishes and $N(s) = N_0$. Each solution is periodic of period $2K(M)s/U$, where K is the complete elliptic integral of the first kind (cf. Ref. 13), and M is the parameter and U the argument of the Jacobian elliptic function which is proportional to s. It can be shown that the zones A and B are equivalent in the sense that for a given supercurrent J, and for each N_{0A} such that $\{N_{0A}, J\}$ belongs to zone A, there exists a value N_{0B} with $\{N_{0B}, J\}$ in zone B, such that N_{0A} is the maximum and N_{0B} the minimum of the same function $N(s)$.

(ii) If $N_0 = 0$,[8] one still has $N_0' = 0$. In addition, Eqs. (10), (12), and (13) show that $J = J_0 = J_1 = 0$. Elementary algebra gives the relation $N_0'' = (N_0')^2/(2N_0)$, and Eqs. (14) and (15) reduce to $\Delta^2 = 1$ and $2\gamma^2 = \sqrt{N_0''}$. Since, in contrast to case (i), N_0'' is now undetermined, we are free to choose $2\gamma^2 > 1$, in which case the form of solution given under D is valid.

This means that infinitely many solutions for R are associated with the pair $\{N_0, J\} = \{0, 0\}$, while only one solution R corresponds to any other value of $\{N_0 \neq 0, J\}$.

It should be noted that this description is valid for general one-dimensional systems. For a micronet with t branches, two parameters $\{N_{0k}, J_k\}$ are associated with each branch k. Hence the total number of dimensions of the parameter space of the micronet is $2t$. For a given temperature T and a given flux Φ, only a finite number of multiplets $\{N_{01}, J_1, ..., N_{0t}, J_t\}$ will satisfy the boundary conditions of the micronet (see Sec. V).

IV. EVALUATION OF THE GIBBS ENERGY

In Eq. (1), the kinetic contribution $|\hat{p}\varphi|^2$ can be integrated by parts over the whole space, leaving in the integral a term of the form $\varphi^*(\hat{p}^2\varphi)$. Equation (3) is then introduced in Eq. (1) and the only term remaining from both the kinetic and the condensation energy is $-(|\alpha|^2/2\beta)N^2$. This shows that this energy contribution is always negative.

In a bulk sample where $\varphi = 1$, the critical magnetic field $H_c(T)$ destroys superconductivity. Hence

$$\frac{|\alpha|^2}{2\beta} = \frac{\mu_0}{2}H_c^2. \tag{16}$$

Extracting the factor $|\alpha|^2/2\beta$ from Eq. (1) reduces the latter to

$$\Delta G = \xi^3 \frac{|\alpha|^2}{2\beta}\int d^3x \left\{-N^2 + \frac{H_{\mathrm{ind}}^2}{H_c^2}\right\}. \tag{17}$$

In the case of a linear singly connected conductor, the second term of ΔG can be expressed as

$$\Delta G_{\mathrm{mag}} = \frac{1}{H_c^2}\int d^3x H_{\mathrm{ind}}^2 = \frac{e^2|\varphi_\infty|^4\hbar^2}{m^2\xi^2}\frac{1}{H_c^2}\frac{L}{\mu_0}(\pi\tilde{a}^2)^2J^2, \tag{18}$$

where $\tilde{a}$ is the radius of the wire, L is the inductance of the circuit, and the prefactor comes from Eq. (4). For a circular loop of quarter perimeter $\tilde{l}$,

$$L = \mu_0\frac{2\tilde{l}}{\pi}\left[\ln\left(\frac{16\tilde{l}}{\pi\tilde{a}}\right) - 1.75\right]. \tag{19}$$

As $0 \le N \le 1$ and N is confined to the wire, the integral of $-N^2$ in Eq. (17) over the whole space is of order $4\tilde{l}\pi\tilde{a}^2$, while the order of ΔG_{mag} is $\tilde{l}(\pi\tilde{a}^2)^2\ln(16\tilde{l}/\pi\tilde{a})$. This estimate shows that in the limit $\tilde{a} \to 0$, ΔG_{mag} decreases to zero faster than the integral of $-N^2$. A straight computation of the different quantities in ΔG_{mag}, evaluated for

aluminum, shows that for $\tilde{a} < 10^{-1}$ μm and $0 \leq J \leq 0.5$ (see Sec. V C), the magnetic energy is equal to a small percentage of the total Gibbs energy at any temperature.

V. STUDY OF THE WHEATSTONE BRIDGE

We suppose that the center of the central branch of the Wheatstone bridge is a center of inversion symmetry (see Fig. 1). Two parameters describe the geometry, l and δ: The first is the normalized half-length of the central branch and the second is the ratio of the normalized half-lengths of the lateral branches to the normalized half-length of the central branch. The normalized curvilinear abscissa is measured from the center of each branch. Figure 1 shows the case where the loops are squares of side $2l$, that is, $\delta = 3$.

For any micronet, the way in which the values of N on different branches match at a node gives a set of equations which determine the solution for a given temperature and a fixed magnetic flux. As the junctions are homogeneous, N cannot exhibit any irregularity at a node. Hence, a first boundary condition follows:

$$\lim_{s \to s_D} N_k(s) = N_D, \tag{20}$$

where k specifies the branch in question connected to a given node D. Since the supercurrent J is conserved a second boundary condition, which is, in fact, Kirchhoff's law, applies,

$$\sum_k J_k = 0, \tag{21}$$

for each node. A third boundary condition concerns the imaginary part I of the complex current density P defined by

$$P = \varphi^* \hat{p} \varphi \tag{22}$$

and requires

$$\lim_{s \to s_D} \sum_k I_k(s) = 0. \tag{23}$$

This last condition is derived in the Appendix.

A. Determination of the second-order phase transition

First we compute the phase transition line of the Wheatstone bridge in the parameter plane $\{l, \Phi/\Phi_0\}$. This line was first obtained by Riess,[14] but we recalculate this line which is needed for the subsequent nonlinear analysis. As the transition is of second order, the order parameter vanishes at the transition and an expression for φ can be obtained by neglecting the term $|\varphi|^2\varphi$ in the GL equation (3). This yields the linearized equation

$$\left(i\frac{\partial}{\partial s} + A_k\right)^2 \varphi_k - \varphi_k = 0, \quad k = l, d, r, \tag{24}$$

where the subscripts l, d, and r designate, respectively, the left, central, and right branches and A_k is the component of the vector potential parallel to the wire along the branch. A gauge can be chosen such that A_k is a constant along every branch and zero in the central branch. Thus

$$A_d = 0 \qquad \text{and} \qquad A_r = -A_l. \tag{25}$$

The solutions of Eq. (24) can be expressed as a linear combination of the four terms obtained by taking all sign combinations indicated in $\exp\{i[A_k(\pm\ell_k - s) + (\ell_k \pm s)]\}$ which takes the value $\varphi_A = |\varphi_A|e^{i\alpha}$ at node A, where $s = -\ell_k$ and $\varphi_B = |\varphi_B|e^{i\beta}$ at node B, where $s = \ell_k$; hence, Eq. (20) is automatically satisfied. To take into account the two other boundary conditions, Eqs. (21) and (23), the currents in each branch must be computed first. One obtains[14]

$$J_k = -|\varphi_A||\varphi_B|\frac{\sin(\alpha - \beta + 2A_k\ell_k)}{\sin(\ell_k)}, \qquad k = l, d, r, \tag{26}$$

$$I_k(s) = \frac{1}{2\sin^2(2\ell_k)}\{|\varphi_A|^2 \sin[2(\ell_k - s)] - |\varphi_B|^2 \sin[2(\ell_k + s)] + 2|\varphi_A||\varphi_B|\cos(\alpha - \beta + 2A_k\ell_k)\sin(2s)\}, \quad k = l, d, r, \tag{27}$$

which must be evaluated at $s = -\ell_k$ and at $s = \ell_k$. Using Eqs. (26) and (27), the set of conditions Eqs. (21) and (23) reduces to two linear equations for φ_A and φ_B. These equations have nontrivial solutions if

$$Q^2 - P^2 = 0, \tag{28}$$

where

$$Q = 2\cot(2\delta l) + \cot(2l), \tag{29}$$

$$P = \frac{2\cos(2\pi\Phi/\Phi_0)}{\sin(2\delta l)} + \frac{1}{\sin(2l)}. \tag{30}$$

These solutions are $\varphi_A = \varphi_B$ when $Q = P$ and $\varphi_A = -\varphi_B$ when $Q = -P$. If we consider Eq. (28) as an implicit function of l vs Φ/Φ_0, we may represent l by an even number of curves, corresponding to $\varphi_A = \varphi_B$ and $\varphi_A = -\varphi_B$, which give it as a function of Φ/Φ_0 of period unity. For $\delta = 1$ there are two curves, as first calculated by Fink.[8] For $\delta = 3$ the corresponding six curves are shown in Fig. 3.

For any flux, the phase transition happens at the smallest value of l satisfying Eq. (28) (heavy line). It can easily be seen that when Φ/Φ_0 vanishes, $l = 0$ is always a solution of $Q = P$. This implies that the symmetrical

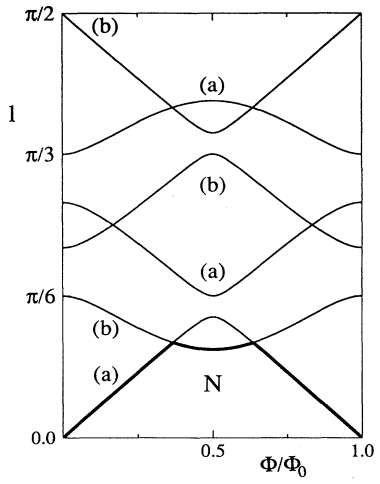

FIG. 3. First period (i.e., $0 \leq \Phi/\Phi_0 \leq 1.0$) of the phase diagram for a Wheatstone bridge with $\delta = 3$ (cf. caption of Fig. 1). These curves are solutions of Eq. (28) which follows from the linearized GL equation. They show those values of the normalized length $l(T)$ where, at flux Φ/Φ_0, the sc order parameter φ can vanish and induce a second-order phase transition. $l(T)$ is related to the temperature by $l(T) = \tilde{l}/\xi(T)$ where $\tilde{l}$ is the half-length of the central branch and $\xi(T)$ the coherence length of the material at temperature T. Φ_0 is the flux quantum. The curves (a) and (b) correspond to the $\varphi_A = \varphi_B$ and $\varphi_A = -\varphi_B$ configurations, respectively. For a given flux Φ in one of the loops of the Wheatstone bridge, the sc phase transition occurs at the lowest curve (bold line) of the diagram. The sc phase exists above this line. N: normal phase.

solution $\varphi_A = \varphi_B$ is realized in zero flux. A change of the configuration of the order parameter occurs when the lowest $\varphi_A = \varphi_B$ curve intersects the lowest $\varphi_A = -\varphi_B$ curve (see Fig. 3), i.e., when Q and P simultaneously vanish. Such a change is found for $\delta = 1, 2, 3$ showing that, at the sc transition for $\Phi/\Phi_0 = 1/2$, the configuration $\varphi_A = -\varphi_B$ appears. From Eq. (26), it can be seen that the current J_d in the central branch is zero. Since $N \neq 0$, from Eq. (7) we see that the gauge-invariant phase θ_d of the order parameter is constant along this branch. This means that in the case $\varphi_A = -\varphi_B$, N must vanish somewhere along the central branch. The currents flow only within the lateral branches; hence they are screening currents. Assuming that φ depends smoothly on the temperature and magnetic flux in the vicinity of the phase transition, this observation serves as a useful guide for the following investigation of the nonlinear case.

B. Approximate study for $1 - T/T_c \ll 1$

1. *Basis of the approximation*

The purpose of this subsection is to evaluate the GL order parameter φ approximately for $T \approx T_c$. In the vicinity of the critical temperature, the coherence length ξ tends to infinity; thus l decreases to zero and our approximation $1 - T/T_c \ll 1$ corresponds to $l \ll 1$. Over a short distance, a strong variation of $R(s)$ [see Eq. (8)] would mean a large increase in the GL free energy. Hence the term of order 3 of R in Eq. (9) can be neglected. The equation to be solved becomes

$$R'^2 = 2(2a_0^2 R + N_0)R, \tag{31}$$

which gives[10]

$$R(s) = \frac{N_0''}{2a_0^2}\sinh^2[a_0(s - s_0)] \cong \frac{1}{2}N_0''(s - s_0)^2. \tag{32}$$

The geometry of the Wheatstone bridge suggests some symmetries for the order parameter.

(1) The squared modulus of the order parameter reaches an extremum N_{0k} at the center of each branch, $k = l, d, r$.

(2) The squared modulus of the order parameter obeys the relationship $N_k(s) = N_k(-s)$, $k = l, d, r$; hence both nodes are equivalent.

Assuming these symmetries, the boundary conditions, Eqs. (20), (21), and (23), are

$$N_d(l) = N_r(\delta l) = N_l(\delta l), \tag{33}$$

$$J_d + J_r + J_l = 0, \tag{34}$$

and

$$N_d'(l) + N_r'(\delta l) + N_l'(\delta l) = 0. \tag{35}$$

2. *Symmetrical solution*

The symmetrical case occurs when

$$N_r(s) = N_l(s), \tag{36}$$

which yields [see Eqs. (34) and (25)]

$$J_r = -J_l \quad \text{and} \quad J_d = 0. \tag{37}$$

Equations (33)–(35) yield the values of N_{0r}, N_{0d}'', N_{0r}'' as functions of N_{0d} and imply that N_{0d} is a maximum when $N(s)$ is convex in the lateral branches. The total flux Φ associated with these configurations can be computed using the fluxoid quantization, which, with our normalization, is expressed as

$$\oint \frac{J(s)}{N(s)}ds = 2\pi l\chi, \tag{38}$$

where

$$\chi = \frac{1}{l}\left(n + \frac{\Phi}{\Phi_0}\right). \tag{39}$$

$J(s)$ is a constant along a branch, but may vary from

branch to branch. Following Eqs. (38) and (39), the phase diagram expressed in terms of Φ/Φ_0 is periodic with period 1 and it is symmetric with respect to $\Phi = 0$. Therefore certain functions, such as the energy or N, are periodic and symmetric, while others, like the current, are periodic but antisymmetric with respect to Φ/Φ_0.

It follows from the symmetries expressed by Eqs. (36) and (37) that the computation of the flux can be restricted to one of the loops and the only contribution to the left-hand side of Eq. (38) is provided by the lateral branch. Retaining only the term of lowest order in l gives

$$N_{0d} = 1 - \frac{\pi^2\chi^2}{\delta(\delta + 1/2)}. \tag{40}$$

The phase diagram is constructed using Eq. (40), N_{0d} being expressed as a function of the flux and of the temperature through χ. When the flux is zero, N_{0d} is maximal, and when N_{0d} vanishes (i.e., at the second-order phase transition), the flux is proportional to l. This is compatible with the solution $\varphi_A = \varphi_B$ of Eq. (28). The screening current flowing through the lateral branches is

$$J_r = \pm J_{0d}\sqrt{1 + 1/(2\delta)}, \tag{41}$$

where J_0 is defined by Eq. (12). Equations (41) and (12) yield $J_r = 0$ for a vanishing flux or along the phase transition line and J_r reaches its maximum for a flux $\Phi(l(T))$ determined by

$$\chi^2 = \frac{\delta(\delta + 1/2)}{3\pi^2}. \tag{42}$$

3. *Solutions $N_r(s) \neq N_l(s)$*

Dropping the symmetry condition imposed by Eq. (36) leads to a magnetostatic problem.[15] If a flux Φ_a is applied to a superconductor, a physical current density J^p appears and, according to Lenz's law, induces a magnetic field which modifies the flux. As the currents are not the same in both lateral branches, the total fluxes will be different in each loop. Hence, the total flux Φ enclosed by a current loop is composed of two terms: the applied flux Φ_a and the induced flux. The latter is the sum of the product of the inductance L_m with the physical net current $j^p_m = \pi\tilde{a}^2 J^p_m$ of each branch (indexed by m) of the loop. With our normalization (see Sec. II), this is expressed by

$$\chi = \chi_a + \sum_m \gamma_m J_m. \tag{43}$$

Here J_m is the normalized current density along branch m, $\chi_a = l^{-1}(n + \Phi_a/\Phi_0)$, and $\gamma^{-1} = 2\pi l\mu_0\lambda^2/(LS)$, where λ is the penetration depth of the material and S is the normalized cross section of the wire.

In the asymmetric case, the fluxoid quantization has to be applied separately in each loop of the micronet and Eq. (38) has to be satisfied. Identifying the total flux Φ and the current J in Eq. (43) with the corresponding quantities in Eq. (38) gives the desired relations between the variables.

Using these results, the general case described by Eqs. (33)–(35) may now be treated. To allow for the conservation of the real currents, we set

$$J_d = J, \tag{44}$$
$$J_r = J/2 + J_e, \tag{45}$$
$$J_l = J/2 - J_e. \tag{46}$$

Introduced into Eqs. (33) and (35), these definitions supply a first relation between the currents,

$$(1 + \delta/2)J^2 + 2\delta J_e^2 - (2\delta + 1)J_{0r}^2 = 0, \tag{47}$$

where J_0 is defined in Eq. (12). Fluxoid quantization [Eq. (38)] gives a first expression for χ_r and χ_l:

$$N_{0r}\pi\chi_r = (1 + \delta/2)J + \delta J_e, \tag{48}$$
$$N_{0r}\pi\chi_l = -(1 + \delta/2)J + \delta J_e, \tag{49}$$

and Eq. (43) yields

$$\chi_r = \chi_a + \gamma_d J + \gamma_r(J_e + J/2), \tag{50}$$
$$\chi_l = \chi_a - \gamma_d J + \gamma_r(J_e - J/2). \tag{51}$$

Expressing χ_r and χ_l in terms of χ_a and N_{0r} gives

$$\chi_r = \chi_l = \chi_a \frac{\delta}{\delta - \gamma_r\pi N_{0r}}. \tag{52}$$

Hence $J = 0$ and thus the highly symmetrical case is reproduced. What has been gained is a relation between the applied flux Φ_a, which enters via χ_a, and the lateral branch current density $J_r = -J_l = J_e$ which can be useful in experiment:

$$J_e = \chi_a \frac{N_{0r}\pi}{\delta - \gamma_r\pi N_{0r}}, \tag{53}$$

where N_{0r} is that solution of

$$-N_{0r}^3\gamma_r^2\pi^2 + N_{0r}^2(\gamma_r^2\pi^2 + 2\gamma_r\pi\delta) + N_{0r}(-2\gamma_r\pi\delta - \delta^2) + \frac{2\delta}{2\delta + 1}\pi^2\chi_a^2 = 0 \tag{54}$$

which lies in the interval $[0, 1]$.

C. Exact solution of the nonlinear problem

Using the formulas given in Table I for $R(s)$ (see Sec. III) and choosing one of the configurations $\varphi_A = \pm\varphi_B$ which appears at the phase transition, Eqs. (20), (21), and (23), describing the boundary conditions, can be numerically solved for chosen values of δ and T.

The boundary conditions specify a solution line in the three-dimensional space of the parameters $\{N_{0r}, N_{0d}, J\}$. For each point of this line, the total flux[16] is determined by integrating JN^{-1} over the whole micronet [cf. Eq. (38)], and the Gibbs energy ΔG is computed as the integral of $-N^2/2$ over the whole micronet (see Sec. IV).

Fink[8] presented the numerical results obtained for the yin-yang geometry ($\delta = 1$) for a single temperature corresponding to $l(T) = 0.71$. [With his parameter choice, this

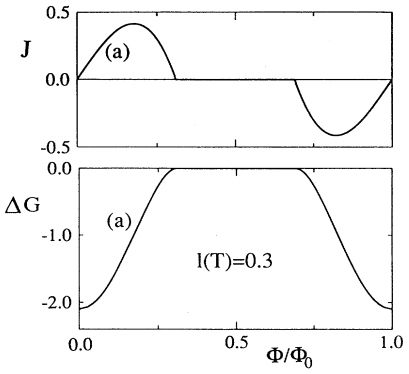

FIG. 4. Normalized current J and Gibbs energy ΔG in terms of the total flux Φ/Φ_0 for the $\delta = 3$ Wheatstone bridge (cf. Fig. 1) at a temperature $T(l = 0.3)$. The unit of ΔG is $|\alpha(T(l = 0.3))|^2/\beta$. Only the first period of the phase diagram is shown (cf. Fig. 3). Only the $\varphi_A = \varphi_B$ configuration occurs. Notice that in a region centered at $\Phi/\Phi_0 = 1/2$ the normal phase is the energetically most favorable one.

corresponds, in Fink's notation, to $R(T) = 2l(T)/\pi = 0.45$.] We show graphs for the double-square $\delta = 3$ geometry at three different $l(T)$, i.e., three different temperatures: in Fig. 4 for $l(T) = 0.3$, in Fig. 5 for $l(T) = 0.5$, and in Fig. 6 for $l(T) = 1.0$.

At $l(T) = 0.3$, only the configuration $\varphi_A = \varphi_B$ appears. As can be seen from Fig. 3, for this value of $l(T)$ the system is normal for fluxes such that $0.31 \leq \Phi/\Phi_0 \leq 0.69$. This is confirmed in Fig. 4 by the vanishing of ΔG and J in that region.

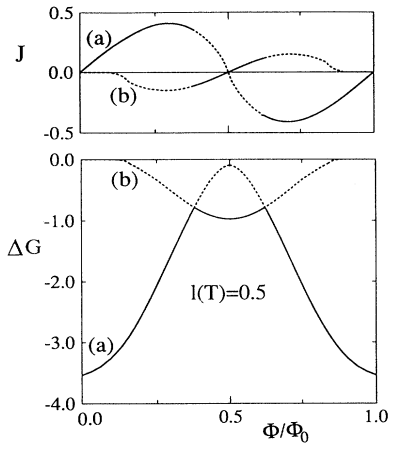

FIG. 5. Normalized currents J and Gibbs energies ΔG in terms of the total flux Φ/Φ_0 for the $\delta = 3$ Wheatstone bridge (cf. Fig. 1) at a temperature $T(l = 0.5)$. The unit of ΔG is $|\alpha[T(l = 0.5)]|^2/\beta$. Only the first period of the phase diagram is shown (cf. Fig. 3). Curves (a) and (b) refer to the $\varphi_A = \varphi_B$ and $\varphi_A = -\varphi_B$ configurations, respectively. In the limit where the self-inductance of the circuit $L \to 0$ and at the flux where the two ΔG curves intersect, a first-order transition occurs between the two configurations (a) and (b) and the current suddenly changes sign and amplitude. The dashed line represents the states of higher free energy.

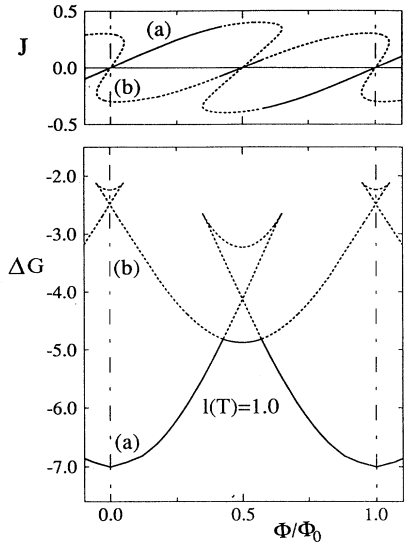

FIG. 6. The same as in Fig. 5, for $T(l = 1.0)$.

For both $l(T) = 0.5$ and $l(T) = 1.0$ (Figs. 5 and 6), the $\delta = 3$ Wheatstone bridge remains superconducting for any value of the flux. Besides the $\varphi_A = \varphi_B$ configuration, the $\varphi_A = -\varphi_B$ configuration also appears for a certain range of the flux. The Gibbs energy ΔG of this configuration is minimal for $\Phi/\Phi_0 = n + 1/2$ and maximal for $\Phi/\Phi_0 = n$, which is the opposite of the behavior of ΔG for $\varphi_A = \varphi_B$. For $\Phi/\Phi_0 = n/2$ (n integer), $J = 0$, and at this value of the flux, the direction of the current reverses.

When, at the same applied flux Φ_a, the curves of ΔG vs Φ_a of both configurations intersect, a transition occurs. In the limit where the inductance L of the micronet tends to zero, the total flux reduces to the applied flux and the Figs. 5 and 6 can be directly exploited to determine which configuration has the lowest energy for any flux. At the flux at which the change of configuration takes place, there is a discontinuity in the slope of ΔG and neither N nor the screening current is continuous. Thus the transition is of first order.

VI. CONCLUSIONS

First we have computed the sc-normal second-order phase transition line $T_c(\Phi)$ of the Wheatstone bridge (Fig. 1) which in the phase diagram $\{l(T), \Phi/\Phi_0\}$ is periodic in Φ/Φ_0 of period 1. [$l(T)$ is defined as the ratio of the half length of the central branch $\tilde{l}$ to the coherence length of the bulk material $\xi(T)$.] This transition line is obtained analytically in the first period of the phase diagram from the linearized GL equation for any value of the ratio δ of the lengths of the lateral branches to that of the central branch (cf. Sec. V A and Fig. 3 for $\delta = 3$). This calculation determines the region of the $\{l(T), \Phi/\Phi_0\}$ phase diagram where superconductivity exists and shows that only two types of configuration of the order parameter are possible at this transition:

(1) $\varphi_A = \varphi_B$ characterized by a maximum of the squared modulus of the sc order parameter at the center of the central branch, while the squared moduli of the order parameters in the lateral branches are equal and convex functions of the distance from a node. For any value of δ, this is realized for fluxes $\Phi/\Phi_0 = n$, where n is an integer.

(2) $\varphi_A = -\varphi_B$ characterized by equal and concave squared moduli of the order parameters in the lateral branches. The squared modulus of the order parameter at the center of the central branch vanishes, while the phase of the order parameter shifts by π at this point. In the cases where the ratio of the lengths of a lateral to the central branch is $\delta = 1, 2, 3$, this configuration is realized for fluxes $\Phi/\Phi_0 = n + 1/2$, where n is an integer.

In the central branch, and for both configurations, the phase of the order parameter is constant (except for the unconsequential phase shift in the $\varphi_A = -\varphi_B$ configuration), and the electromagnetic vector potential vanishes. This implies that only screening currents can appear at the second-order phase transition; i.e., the current in the central branch is zero.

For $1 - T/T_c \ll 1$, our approximate analytical study (Sec. V B) has shown that only the $\varphi_A = \varphi_B$ configuration exists in the sc phase corresponding to small fluxes.

In Sec. V C, the analytical solution of the nonlinear GL equation has been numerically adjusted to fit the boundary conditions of a particular Wheatstone bridge with $\delta = 3$. We have restricted our investigation to the $\varphi_A = \varphi_B$ and $\varphi_A = -\varphi_B$ configurations and have obtained graphs for the normalized currents J and the Gibbs energy ΔG in terms of the total flux for $l(T) = 0.3$, $l(T) = 0.5$, and $l(T) = 1.0$ (Figs. 4, 5, and 6).

For $l(T) = 0.3$ (Fig. 4), the normal state subsists for fluxes in the interval $0.31 \leq \Phi/\Phi_0 \leq 0.69$ and only the $\varphi_A = \varphi_B$ configuration appears. For $l(T) = 0.5$ and $l(T) = 1.0$ the system remains superconducting whatever the flux. For these values of $l(T)$, both $\varphi_A = \pm\varphi_B$ configurations appear, and in the limit where the inductance L of the micronet tends to zero (i.e., the total flux reduces to the applied flux and the magnetic energy of the net is zero), the figures show that the curves of the Gibbs energy vs flux of both configurations intersect. This means that at this flux, a transition occurs between the two configurations. Since the order parameter and the supercurrent are discontinuous functions at this value of the flux, the transition is of first order.

In the case $\Phi/\Phi_0 = n/2$, with n an integer, $J = 0$ and no magnetic energy contributes to ΔG. For these fluxes, the values of ΔG presented in the figures are exact for any diameter of the wires. When $J \neq 0$, the magnetic energy should be included for finite diameter wires. For the experimental values of the diameter given at the end of Sec. IV, the magnetic energy is equal to a small percentage of the total Gibbs energy.

We have shown (see, e.g., Figs. 3, 5, and 6) that, even though the temperature is different, the sequence of configurations of the order parameter as a function of the flux found at the sc second-order phase transition remains the same. These results for a $\delta = 3$ Wheatstone bridge are in good agreement with the theoretical findings of Fink for the case $\delta = 1$.[8]

The above results lend trustworthiness to the linear approach. As we have seen, no qualitatively significant modifications are brought about by the nonlinear development. This is an important point since, at present, interest is directed toward different other geometries of sc micronets such as periodic structures.[17,18] Experimental techniques like decoration,[19] developed to study the physical properties of micronets, may provide tests of the theory.

Of special interest would be an experimental test of the discontinuous change of the direction of the supercurrent as a function of the flux, as predicted in Sec. V C.

ACKNOWLEDGMENTS

The authors thank Dr. Z. Domański, Dr. F. Pázmándi, and Professor H. J. Fink for useful discussions. The support of the Swiss National Science Foundation through Grant No. 20-37642.93 is gratefully acknowledged.

APPENDIX: BOUNDARY CONDITIONS

The third boundary condition introduced in Sec. V concerns the imaginary part I of the complex current density P defined by

$$P = \varphi^* \hat{p} \varphi = J + iI. \tag{A1}$$

Using the three-dimensional version of Eq. (3),

$$\hat{p}^2 \varphi = (1 - N)\varphi, \tag{A2}$$

it follows from Eq. (A1) that

$$\nabla \cdot P = i(-|\hat{p}\varphi|^2 + N - N^2) = i \nabla \cdot I. \tag{A3}$$

On the other hand, taking the divergence of Eq. (A1), and noting that there is no normal current in the net, and we deal with a static system, the divergence of J vanishes. This confirms in another way the absence of a real part in the expression (A3).

Gauss's theorem applied to $\nabla \cdot P$ on a macroscopic node (cf. Fig. 7) gives

$$\int_V \nabla \cdot P d^3x = i \int_S I \cdot d\sigma, \tag{A4}$$

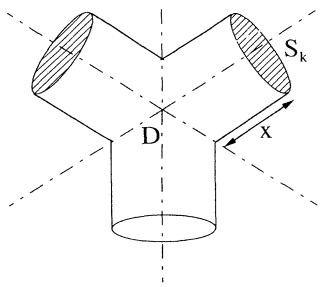

FIG. 7. Schematic diagram of a truncated macroscopic node.

where V is the volume of the body obtained by truncating all wires at a distance x from the node which is inside V, and S is the surface enclosing V.

When the length x of the branches diminishes, $V \to 0$, and if we assume that $\nabla \cdot P$ has no singularity, the integral over the volume vanishes. The only contributions to the surface integral come from the sections S_k. Assuming that the imaginary current densities I_k are one dimensional, we obtain

$$\lim_{s \to s_D} \sum_k I_k(s) = 0, \tag{A5}$$

which is the third boundary condition.

[1] P.-G. de Gennes, C.R. Acad. Sci. Paris **292**, 279 (1981).
[2] S. Alexander, Phys. Rev. B **27**, 1541 (1983).
[3] J. Simonin, D. Rodrigues, and A. López, Phys. Rev. Lett. **49**, 944 (1982).
[4] H. J. Fink, A. López, and R. Maynard, Phys. Rev. B **26**, 5237 (1982).
[5] H. J. Fink and V. Grünfeld, Phys. Rev. B **31**, 600 (1985).
[6] H. J. Fink, V. Grünfeld, and A. López, Phys. Rev. B **35**, 35 (1987); H. J. Fink, J. Loo, and S. M. Roberts, *ibid.* **37**, 5050 (1988).
[7] V. V. Moshchalkov *et al.,* Nature **361**, 620 (1993).
[8] H. J. Fink, Phys. Rev. B **45**, 4799 (1992); **48**, 3579 (1993).
[9] M. Tinkham, *Introduction to Superconductivity* (McGraw-Hill, New York, 1975).
[10] H. J. Fink and S. B. Haley, Phys. Rev. B **43**, 10151 (1991).
[11] This table is constructed on the basis of Ref. 12.
[12] S. B. Haley and H. J. Fink (unpublished).
[13] *Handbook of Mathematical Functions,* 9th ed., edited by M. Abramowitz and I. A. Stegun, Natl. Bur. Stand. Appl. Math. Ser. No. 55 (U.S. GPO, Washington, D.C., 1970).
[14] J. Riess, J. Phys. (Paris) Lett. **43**, L-277 (1982).
[15] H. J. Fink and V. Grünfeld, Phys. Rev. B **33**, 6088 (1986).
[16] The inductance L diverges when the radius $\tilde{a}$ of the wires vanishes [see Eq. (19)]. This property of L does not depend on the geometry of the micronet. Hence a computation of the applied flux Φ_a in terms of the normalized current J and of the total flux Φ would depend drastically on the values chosen for $\tilde{l}$ and $\tilde{a}$. Therefore we prefer to use the total flux instead of the applied flux as abscissa in the graphs.
[17] Y. Y. Wang, R. Rammal, and B. Pannetier, J. Low Temp. Phys. **68**, 301 (1987).
[18] T. Larson, S. Haley, and P. Erdös, Physica B **194**, 1425 (1994).
[19] K. Runge and B. Pannetier, Europhys. Lett. **24**, 737 (1993).